

$T = 293$  K,  $Z = 4$ , reflections collected/unique: 9438/3824 ( $R_{\text{int}} = 0.0457$ ), no observation [ $I > 2\sigma(I)$ ] 3824, parameters 257. CCDC-190370 (**5g**) contains the supplementary crystallographic data for this paper. These data can be obtained free of charge via [www.ccdc.cam.ac.uk/conts/retrieving.html](http://www.ccdc.cam.ac.uk/conts/retrieving.html) (or from the Cambridge Crystallographic Data Centre, 12, Union Road, Cambridge CB21EZ, UK; fax: (+44) 1223-336-033; or deposit @ccdc.cam.ac.uk).

[17] S. Ma, B. Xu, B. Ni, *J. Org. Chem.* **2000**, *65*, 8532.

## Electrochemical Sensors

### Mono-Tetrathiafulvalene Calix[4]pyrrole in the Electrochemical Sensing of Anions\*\*

Kent A. Nielsen, Jan O. Jeppesen,\* Eric Levillain, and Jan Becher\*

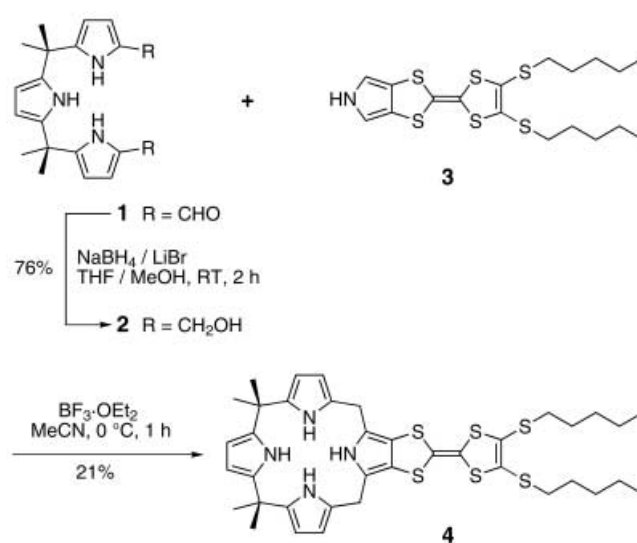
Dedicated to Professor J. Fraser Stoddart  
on the occasion of his 60th birthday

The advent of supramolecular chemistry<sup>[1]</sup> has stimulated the contemporary chemist's interest in the development of chemosensors capable of recognizing specific chemical species.<sup>[2]</sup> Calix[4]pyrroles<sup>[3]</sup>—first synthesized in the 19th Century by Baeyer<sup>[4]</sup>—contain four pyrrole–NH hydrogen-bond functionalities and have recently been studied for possible use as receptors for anionic and neutral substrates.<sup>[5]</sup> They have been used to prepare optical anion sensors<sup>[6]</sup> and anion-selective high-performance liquid-chromatography (HPLC) supports.<sup>[7]</sup> However, only a few electrochemically active sensors based on calix[4]pyrroles have been reported.<sup>[8]</sup> Electrochemically active sensors, designed to permit the detection of substrates by binding-induced changes in the redox properties, are generally composed of a receptor unit, which works by the covalent association of a substrate-recognition functionality, and an electrochemical-signaling capacity (redox-active unit). The redox-active tetrathiafulvalene<sup>[9]</sup> (TTF) unit can exist in three stable redox states (TTF<sup>0</sup>,

TTF<sup>+</sup>, and TTF<sup>2+</sup>) and for this reason TTF derivatives have found widespread use in materials chemistry.<sup>[9]</sup> Progress in synthetic TTF chemistry<sup>[9]</sup> has revolutionized the possibilities for the incorporation of TTF into macrocyclic, molecular, and supramolecular structures and has transformed complicated systems, such as TTF cyclophanes,<sup>[9]</sup> TTF catenanes,<sup>[9]</sup> and TTF rotaxanes/pseudorotaxanes<sup>[9,10]</sup> from chemical curiosities into a vibrant area of modern-day research. In the context of electrochemically active sensors, TTF has already been used as the redox-active unit in a number of cation responsive receptors.<sup>[11]</sup> However, to our knowledge, no anion receptor incorporating TTF as the redox-active unit has been reported. We have recently developed an efficient synthesis of the parent pyrrolo[3,4-*d*]TTF-ring system.<sup>[12]</sup> With this building block in hand, we have prepared the first example of a single molecule in which the anion-receptor abilities of the calix[4]-pyrrole system were coupled to the favorable redox properties of the TTF core through direct annulation of one TTF unit to the upper rim of the calix[4]pyrrole skeleton.

Herein, we report the synthesis of the first calix[4]pyrrole incorporating a TTF unit. Furthermore, we describe our <sup>1</sup>H NMR spectroscopic and electrochemical studies on the recognition abilities of this novel mono-TTF calix[4]pyrrole **4** system towards anions.

Our preparation of the mono-TTF calix[4]pyrrole **4** is outlined in Scheme 1. The tripyrrane dialdehyde **1** was prepared according to a literature procedure<sup>[13]</sup> by the condensation of pyrrole and acetone followed by a Clezy formylation. The reduction of the formyl groups with NaBH<sub>4</sub>/LiBr in anhydrous THF/MeOH produced the bishydroxymethyltripyrane **2** in 76% yield. The tripyrrane **2** was used immediately after purification by means of flash column chromatography on account of the low stability of the compound. Treatment of equal quantities of **2** and the newly developed pyrrolo TTF **3** with a catalytic amount of BF<sub>3</sub>·Et<sub>2</sub>O in anhydrous MeCN, gave the mono-TTF calix[4]pyrrole **4** as yellow crystals after purification by means of column chromatography (yield 21%).<sup>[14]</sup>



**Scheme 1.** Synthesis of the mono-TTF calix[4]pyrrole **4**.

[\*] Dr. J. O. Jeppesen, Prof. J. Becher, K. A. Nielsen  
Department of Chemistry  
Odense University (University of Southern Denmark)  
Campusvej 55, 5230 Odense M (Denmark)  
Fax: (+45) 66-158-780  
E-mail: [joj@chem.sdu.dk](mailto:joj@chem.sdu.dk)  
[jbe@chem.sdu.dk](mailto:jbe@chem.sdu.dk)

Dr. E. Levillain  
Ingénierie Moléculaire et Matériaux Organiques  
CNRS UMR 6501, Université d'Angers  
2 Bd Lavoisier, 49045 Angers (France)

[\*\*] We gratefully acknowledge the University of Odense for a Ph.D. scholarship to K.A.N., financial support from Carlsbergfondet to J.O.J., and the French Embassy Copenhagen for a travel grant to J.B.

A high-resolution MALDI-MS of **4** showed the exact mass  $m/z$  752.2170, corresponding to  $M^{++}$  (calcd mass  $M^{++}$  752.2198). The  $^1\text{H}$  NMR spectrum (250 MHz) of **4**, recorded in  $\text{CD}_3\text{CN}$  at 303 K, showed three broad singlets at  $\delta = 7.81$ , 7.95, and 8.22 ppm—integrating to 1 H, 1 H, and 2 H, respectively,—which can be assigned to the three sets of chemically nonequivalent NH protons. An  $^1\text{H}$ - $^1\text{H}$ NOE-NMR experiment was carried out to assign the resonance signals associated with the pyrrole NH protons. Irradiation of the *meso*- $\text{CH}_2$  protons ( $\delta = 3.61$  ppm) led to signal enhancements for the signals at  $\delta = 7.95$  and 8.22 ppm, respectively, but no observable effect for the signal at  $\delta = 7.81$  ppm. These results clearly indicate that the resonance signal at  $\delta = 7.95$  ppm corresponds to the NH proton on the pyrrolo-TTF unit, whereas the resonance signal at  $\delta = 7.81$  ppm corresponds to the pyrrole-NH proton opposite to the pyrrolo-TTF unit. Finally, the resonance signal at  $\delta = 8.22$  ppm is assigned to the remaining two chemically equivalent pyrrole-NH protons. Solution oxidation potentials (vs Ag/AgCl) obtained from a cyclic voltammogram of compound **4** recorded in MeCN revealed two pairs of reversible redox waves at  $E_{1/2}^1 = 0.45$  V and  $E_{1/2}^2 = 0.75$  V.

By employing  $^1\text{H}$  NMR spectroscopy and cyclic voltammetry (CV), **4** was shown to form complexes with  $\text{Br}^-$ ,  $\text{Cl}^-$ , and  $\text{F}^-$  ions. A comparison of the  $^1\text{H}$  NMR spectra ( $\text{CD}_3\text{CN}$ , 300 K) of the free receptor **4** (Figure 1 a) and **4** in the presence of  $\text{Br}^-$  ions (Figure 1 b) reveals significant chemical-shift differences for the resonances associated with the NH protons (downfield shifts,  $\Delta\delta = 2.2$ –3.2 ppm), which indicates that the  $\text{Br}^-$  ion is complexed by **4**. A continuous-variation  $^1\text{H}$  NMR experiment was carried out to determine the stoichiometry of the binding between **4** and  $\text{Br}^-$  ions. The Job plot<sup>[15]</sup> obtained exhibit a maximum at 0.55, thus indicating that **4** forms a 1:1 complex with  $\text{Br}^-$  ions. To target biological analytes, the receptor **4** should function in the presence of water. Therefore, binding studies between **4** and  $\text{Br}^-$ ,  $\text{Cl}^-$ , and  $\text{F}^-$  ions were

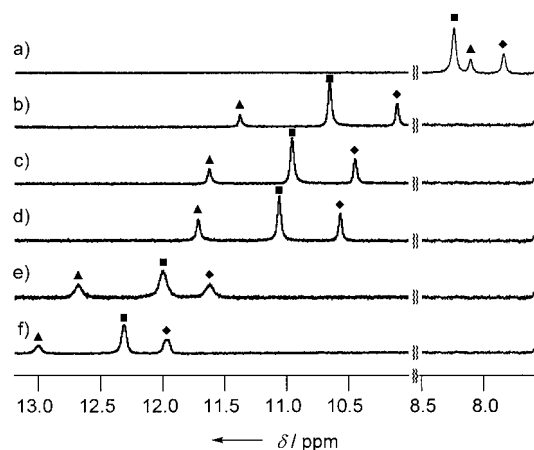


**Figure 1.** Partial  $^1\text{H}$  NMR spectra (300 MHz) recorded in  $\text{CD}_3\text{CN}/0.5\%$  v/v  $\text{D}_2\text{O}$  at 300 K of a) free receptor **4** (3.9 mM), b) **4** +  $\text{Br}^-$  (3.9 equiv), c) **4** +  $\text{Br}^-$  (3.9 equiv) +  $\text{Cl}^-$  (2.1 equiv), d) **4** +  $\text{Cl}^-$  (7.4 equiv), e) **4** +  $\text{Cl}^-$  (7.4 equiv) +  $\text{F}^-$  (2.2 equiv), f) **4** +  $\text{F}^-$  (10.5 equiv). The signals correspond to the three different pyrrole-NH protons.  $\blacktriangle$  = NH on the pyrrolo-TTF unit,  $\blacksquare$  = NH adjacent to the pyrrolo-TTF unit, and  $\blacklozenge$  = NH opposite to the pyrrolo-TTF unit.

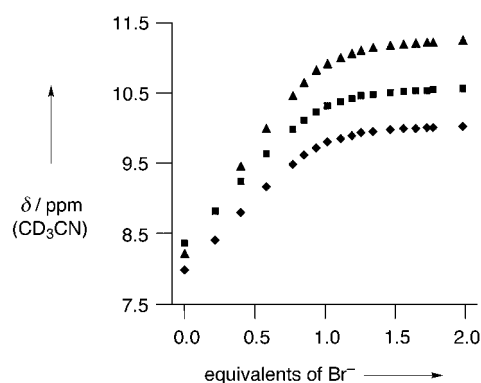


**Figure 2.**  $^1\text{H}$  NMR titration curves of the perturbation of the three non-equivalent NH protons upon addition of increasing amounts of  $\text{Br}^-$  ions.  $\blacktriangle$  = NH on the pyrrolo-TTF unit,  $\blacksquare$  = NH adjacent to the pyrrolo-TTF unit, and  $\blacklozenge$  = NH opposite to the pyrrolo-TTF unit.

performed in  $\text{CD}_3\text{CN}$  containing 0.5% v/v  $\text{D}_2\text{O}$ , as acetonitrile is water miscible, which would allow the receptor **4** to sense anions added in the form of aqueous solutions.<sup>[16]</sup> To determine the binding constant ( $K_a$ ) for the 1:1 complex of  $\text{Br}^-$  ions and **4**,  $^1\text{H}$  NMR titration experiments (Figure 2) were carried out. This was done by means of monitoring the changes in the chemical shift for the resonance signals associated with the three nonequivalent NH protons upon the addition of an increasing amount of  $n\text{Bu}_4\text{NBr}$  to the receptor **4** at 300 K. The binding constant was obtained using the nonlinear curve-fitting program EQNMR<sup>[17]</sup> and gave an average  $K_a$  value of  $7.6 \times 10^3 \text{ M}^{-1}$  for the **4**- $\text{Br}^-$  complex. Similar titration experiments were carried out with solutions containing  $\text{Cl}^-$  and  $\text{F}^-$  ions. However, as a consequence of strong binding between the receptor **4** and these two anions, the titration plots tended towards linearity with increasing anion concentration, which made the nonlinear curve fitting procedure unreliable<sup>[18]</sup> for estimating  $K_a$  values. To determine the  $K_a$  values for the **4**- $\text{Cl}^-$  and **4**- $\text{F}^-$  complex, a competitive  $^1\text{H}$  NMR spectroscopic method was used.<sup>[18]</sup> The binding constant between **4** and  $\text{Cl}^-$  ions was determined in a competitive experiment with  $\text{Br}^-$  ions under conditions of negligible free receptor concentrations. Addition of a solution containing  $\text{Cl}^-$  ions to a solution of **4** saturated with  $\text{Br}^-$  ions induced further downfield shifts (Figure 1 c) of the resonance signals associated with the NH protons, which indicates that complexed  $\text{Br}^-$  has been partly replaced by  $\text{Cl}^-$  ions. Analysis<sup>[18b]</sup> of the data gave a  $K_a$  value of  $1.2 \times 10^5 \text{ M}^{-1}$  for the **4**- $\text{Cl}^-$  complex. A similar competition experiment was carried out between  $\text{F}^-$  and  $\text{Cl}^-$  (Figure 1 e). These results are summarized in Table 1.

The receptor **4** was designed to permit the detection of anions by binding-induced changes in the electrochemically properties of the TTF unit. CV was used to probe the changes in the redox potentials of **4** upon complexation of anions. The progressive addition of a solution containing  $\text{Br}^-$  ions to a solution of **4** in MeCN at 298 K resulted in a cathodic displacement of the first oxidation potential ( $E_{1/2}^1$ ) of the TTF unit (Figure 3). It should be noted (Figure 3 a) that the current intensity associated with second oxidation wave increases as the concentration of  $\text{Br}^-$  ions increases. This unexpected

**Table 1:** Binding constants between **4** and the Br<sup>−</sup>, Cl<sup>−</sup>, and F<sup>−</sup> ions determined by <sup>1</sup>H NMR spectroscopy at 300 K, and first redox potentials E<sub>1/2</sub><sup>1</sup> of the complexes **4**·X<sup>−</sup> (where X is a halide) determined by CV at 298 K.

X <sup>−</sup>	K <sub>a</sub> [M <sup>−1</sup> ] (CD <sub>3</sub> CN/ 0.5 % v/v D <sub>2</sub> O)	E <sub>1/2</sub> <sup>1</sup> [mV] (MeCN) <sup>[a]</sup>	ΔE [mV] (MeCN) <sup>[b]</sup>
Br <sup>−</sup>	7.6 × 10 <sup>3</sup> <sup>[c]</sup>	+467	−34
Cl <sup>−</sup>	1.2 × 10 <sup>5</sup> <sup>[d]</sup>	+462	−43
F <sup>−</sup>	2.1 × 10 <sup>6</sup> <sup>[e]</sup>	—	—

[a] Values obtained from 1:1 mixtures of **4** and *n*Bu<sub>4</sub>NX. [b] Maximum ΔE values (ΔE<sub>max</sub>) were obtained from 1:2 mixtures of **4** and *n*Bu<sub>4</sub>NX. [c] A CD<sub>3</sub>CN (0.5 % v/v D<sub>2</sub>O) solution of receptor **4** (3.9 mM) was titrated by adding a concentrated CD<sub>3</sub>CN (0.5 % v/v D<sub>2</sub>O) solution of *n*Bu<sub>4</sub>NBr which also contained receptor **4** at the initial concentration to account for dilution effects. The binding constant was elucidated using the EQNMR computer program<sup>[17]</sup> and is the average of two independent experiments using the three NH protons as probes, the estimated error was < 10 %. [d] Determined from competitive binding experiments.<sup>[18]</sup> An average K<sub>rel</sub> of 16.8 for the ions Cl<sup>−</sup>/Br<sup>−</sup> was obtained by analyzing a CD<sub>3</sub>CN (0.5 % v/v D<sub>2</sub>O) solution of **4** (3.9 mM) containing Br<sup>−</sup> (3.9 equiv) and Cl<sup>−</sup> (either 1.6 or 2.1 equiv), estimated error was < 15 %. [e] Determined from competitive binding experiments.<sup>[18]</sup> An average K<sub>rel</sub> of 16.9 for F<sup>−</sup>/Cl<sup>−</sup> was obtained by analyzing a CD<sub>3</sub>CN (0.5 % v/v D<sub>2</sub>O) solution of **4** (3.9 mM) containing Cl<sup>−</sup> (7.4 equiv) and F<sup>−</sup> (either 2.0 or 2.2 equiv), estimated error was < 15 %.

growth of the current intensity is a consequence of the oxidation of the anion. Indeed, in the absence of the receptor **4**, the Br<sup>−</sup> ion undergoes oxidation<sup>[19]</sup> in solution at a potential, which is close to the second oxidation potential of **4**. As a consequence of the overlapping nature of these two oxidation processes, it is not possible to obtain any information about whether complexation of the anions to **4** also affect the second oxidation potential of the TTF unit in **4**. It is evident from Figure 3b that the displacement of the first oxidation potential reach a limit (ΔE = −40 mV) when approximately stoichiometric amounts of Br<sup>−</sup> ions were added to **4**, which provides further evidence for the high stability of the **4**·Br<sup>−</sup> complex. Similar cathodic displacements were observed when **4** was titrated with a solution containing Cl<sup>−</sup> ions, and the results obtained are recorded in Table 1,<sup>[20]</sup> together with the results obtained from the titration of **4** with a solution containing Br<sup>−</sup> ions. The results from the electrochemical experiments reveal that the complexation of the anions inside the cavity of **4** shift the first oxidation of the TTF unit towards more cathodic potentials,<sup>[21]</sup> which can be accounted for by delocalization of the negative charge from the binding site N–H···X<sup>−</sup> to the TTF core.<sup>[22]</sup> The annulation of the TTF unit to the upper rim of the calix[4]pyrrole skeleton, not only transduces the binding event to an electrochemical output signal, but also substantially increases the binding abilities of the receptor towards anionic substrates as compared to other calix[4]pyrrole receptors, such as *meso*-octamethylcalix[4]pyrrole.<sup>[23]</sup> To our knowledge, **4** displays the strongest anion binding affinities yet recorded for calix[4]pyrrole receptors, and the binding constants obtained (Table 1) between **4** and Br<sup>−</sup>, Cl<sup>−</sup>, and F<sup>−</sup> ions are two orders of magnitude higher than those reported for *meso*-octamethylcalix[4]pyrrole.<sup>[24]</sup> The stronger affinity of **4** towards

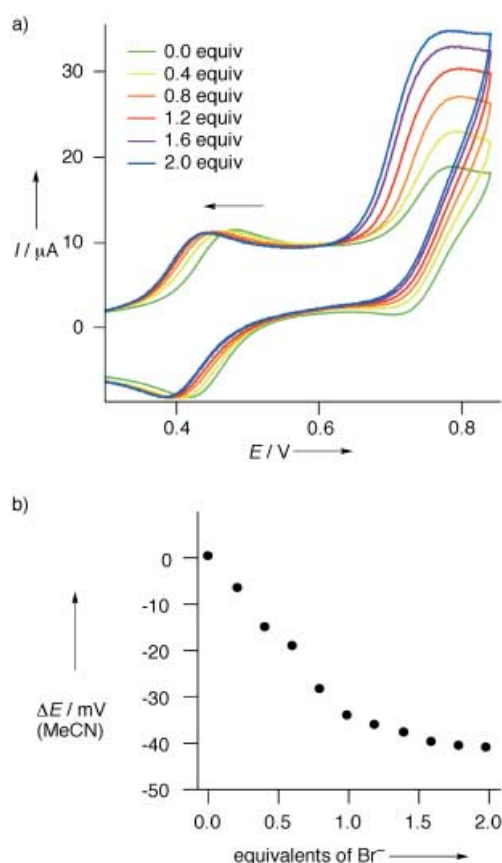


**Figure 3.** a) Cyclic voltammograms of the receptor **4** (0.5 mM) recorded in MeCN at 298 K with *n*Bu<sub>4</sub>NPF<sub>6</sub> (0.4 M) as the supporting electrolyte. Experiments were carried out in a glove box containing anhydrous oxygen-free (< 1 ppm) argon and without light, at a scan rate of 0.5 Vs<sup>−1</sup>.<sup>[25]</sup> The receptor **4** was titrated by adding concentrated MeCN solution of *n*Bu<sub>4</sub>NBr that also contained receptor **4** at the initial concentration, to counter the dilution effects. The potentials were referred to Ag/AgCl. b) CV titration curves showing the cathodic shift of the first oxidation potential of the receptor **4** upon addition of Br<sup>−</sup> ions. Note that the cathodic shift of the first oxidation potential is independent of the second oxidation process.

anions is presumably a direct consequence of the pyrrolo-TTF–NH proton being more acidic than the other NH protons of **4**. This factor implies that the pyrrolo-TTF–NH proton is able to form a stronger hydrogen bond with anions upon complexation, as compared to NH protons in the parent calix[4]pyrrole. This hypothesis is supported by the fact that the pyrrolo-TTF–NH proton experience the largest difference in chemical shift (Δδ) when solutions containing halides are added. In the case of the Br<sup>−</sup> ion, the Δδ reach a value of 3.2 ppm (Figure 2), whereas the remaining pyrrole–NH protons only reach Δδ values in the range of 2.2–2.3 ppm.

In summary, we have prepared an efficient chemosensor—mono-TTF-calix[4]pyrrole **4**—that allows the detection of anions by electrochemical means. The incorporation of one redox-active pyrrolo-TTF unit into a calix[4]pyrrole produces a receptor with the strongest binding affinities toward Br<sup>−</sup>, Cl<sup>−</sup>, and F<sup>−</sup> ions yet recorded for a calix[4]pyrrole system. To our knowledge, **4** represents the first anion sensor based on TTF and the first calix[4]pyrrole system shown to have an

approximately stoichiometric CV response upon the addition of anions. These observations make the redox-responsive calix[4]pyrrole **4** and related systems very attractive for further investigations.

### Experimental Section

**2:** NaBH<sub>4</sub> (79.0 mg, 2.09 mmol) was added in one portion to a solution of the tripyrrane dialdehyde<sup>[13]</sup> **1** (235 mg, 0.70 mmol) and anhydrous LiBr (181 mg, 2.09 mmol) in anhydrous THF-MeOH (70 mL, 2:1 v/v). The reaction mixture was stirred at room temperature for 2 h before H<sub>2</sub>O (50 mL) was added. The mixture was extracted with CH<sub>2</sub>Cl<sub>2</sub> (3 × 50 mL), and the extract was dried (MgSO<sub>4</sub>). The solvent was removed under vacuum and the residue was purified by column chromatography (SiO<sub>2</sub>; PhMe:EtOAc 1:1). The colorless band containing the product (*R*<sub>f</sub> = 0.2) was collected and the solvent evaporated affording the bishydroxymethyl tripyrrane **2** (0.18 g, 76 %) as a colorless solid. The product was used immediately after purification, on account of its low stability: <sup>1</sup>H NMR (CDCl<sub>3</sub>, 300 MHz, 298 K): δ = 1.55 (s, 12H), 2.41 (br, s, 2H), 4.30 (s, 4H), 5.88–5.92 (m, 4H), 5.99 (d, *J* = 2.8 Hz, 2H), 7.55 (br, s, 1H), 8.32 ppm (br, s, 2H); <sup>13</sup>C NMR (CDCl<sub>3</sub>, 75 MHz, 298 K): δ = 29.3, 35.5, 57.7, 103.3, 103.4, 106.7, 130.1, 138.6, 140.6 ppm.

**4:** Tripyrrane **2** (0.17 g, 0.50 mmol) and the pyrrolo-TTF<sup>[12]</sup> **3** (0.22 g, 0.50 mmol) was dissolved in anhydrous MeCN (50 mL) under an atmosphere of nitrogen and stirred at 0 °C for 10 min before a catalytic amount of BF<sub>3</sub>·Et<sub>2</sub>O (4.33 μL, ~5 mg, 5 μmol) was added to the yellow solution. Stirring was maintained for 1 h at 0 °C, the solvent was then removed under reduced pressure, and the resulting residue was dissolved in CH<sub>2</sub>Cl<sub>2</sub> (80 mL), washed with an aqueous NaOH solution (0.1 M, 20 mL) and H<sub>2</sub>O (2 × 30 mL), and dried (MgSO<sub>4</sub>). The solvent was removed under reduced pressure and the resulting yellow solid was subjected to column chromatography (SiO<sub>2</sub>; cyclohexane:CH<sub>2</sub>Cl<sub>2</sub> 2:1). The yellow band containing the product (*R*<sub>f</sub> = 0.3) was collected and the solvent evaporated under vacuum affording the mono-TTF calix[4]pyrrole **4** (79.1 mg, 21 %) as a yellow solid. Recrystallization from CH<sub>2</sub>Cl<sub>2</sub>/n-C<sub>7</sub>H<sub>16</sub> gave **4** as thin yellow needles: m.p. 139.5–140.5 °C; <sup>1</sup>H NMR (CD<sub>3</sub>CN, 250 MHz, 303 K): δ = 0.89 (t, *J* = 6.9 Hz, 6H), 1.25–1.43 (m, 8H), 1.51 (s, 12H), 1.55–1.67 (m, 4H), 2.84 (t, *J* = 7.3 Hz, 4H), 3.61 (s, 4H), 5.73–5.79 (m, 2H), 5.79–5.85 (m, 4H), 7.81 (br, s, 1H), 7.95 (br, s, 1H), 8.22 ppm (br, s, 2H); HiResMALDI: *m/z* 752.2170 (calcd for C<sub>38</sub>H<sub>48</sub>N<sub>4</sub>S<sub>6</sub><sup>+</sup> 752.2198); elemental analysis calcd (%) for C<sub>38</sub>H<sub>48</sub>N<sub>4</sub>S<sub>6</sub> (753.21): C 60.59, H 6.42, N 7.44, S 25.54; found C 60.67, H 6.26, N 7.55, S 25.68.

Received: June 14, 2002

Revised: September 3, 2002 [Z19534]

- [1] a) J.-M. Lehn, *Supramolecular Chemistry*, VCH, Weinheim, **1995**; b) *Comprehensive Supramolecular Chemistry*, Vol. 1–11 (Eds.: J. L. Atwood, J. E. D. Davies, D. D. MacNicol, F. Vögtle, D. Reinhoudt), Pergamon, Oxford, **1996**.
- [2] a) P. L. Boulas, M. Gomez-Kaifer, L. Echegoyen, *Angew. Chem.* **1998**, *110*, 226–258; *Angew. Chem. Int. Ed.* **1998**, *37*, 216–247; b) A. P. Davis, R. S. Wareham, *Angew. Chem.* **1999**, *111*, 3160–3179; *Angew. Chem. Int. Ed.* **1999**, *38*, 2978–2996; c) P. A. Gale, *Coord. Chem. Rev.* **2000**, *199*, 181–233; d) B. Valeur, I. Leray, *Coord. Chem. Rev.* **2000**, *205*, 3–40; e) P. A. Gale, *Coord. Chem. Rev.* **2001**, *213*, 79–128; f) P. D. Beer, P. A. Gale, *Angew. Chem.* **2001**, *113*, 502–532; *Angew. Chem. Int. Ed.* **2001**, *40*, 486–516.
- [3] J. L. Sessler, P. A. Gale in *The Porphyrin Handbook*, Vol. 6 (Eds.: K. M. Kadish, K. M. Smith, R. Guilard), Academic Press, San Diego, **2000**, pp. 257–278.
- [4] A. Baeyer, *Ber. Dtsch. Chem. Ges.* **1886**, *19*, 2184–2185.
- [5] a) P. Anzenbacher, Jr., A. C. Try, H. Miyaji, K. Jursýková, V. M. Lynch, M. Marquez, J. L. Sessler, *J. Am. Chem. Soc.* **2000**, *122*, 10268–10272; b) F. P. Schmidtchen, *Org. Lett.* **2002**, *4*, 431–434; c) D.-W. Yoon, H. Hwang, C.-H. Lee, *Angew. Chem.* **2002**, *114*, 1835–1837; *Angew. Chem. Int. Ed.* **2002**, *41*, 1757–1759.
- [6] H. Miyaji, W. Sato, J. L. Sessler, *Angew. Chem.* **2000**, *112*, 1847–1850; *Angew. Chem. Int. Ed.* **2000**, *39*, 1777–1780.
- [7] J. L. Sessler, P. A. Gale, J. W. Genge, *Chem. Eur. J.* **1998**, *4*, 1095–1099.
- [8] a) J. L. Sessler, A. Gebauer, P. A. Gale, *Gazz. Chim. Ital.* **1997**, *127*, 723–726; b) P. A. Gale, M. B. Hursthouse, M. E. Light, J. L. Sessler, C. N. Warriner, R. S. Zimmerman, *Tetrahedron Lett.* **2001**, *42*, 6759–6762.
- [9] For recent TTF reviews, see: a) M. R. Bryce, *J. Mater. Chem.* **2000**, *10*, 589–598; b) M. B. Nielsen, C. Lomholt, J. Becher, *Chem. Soc. Rev.* **2000**, *29*, 153–164; c) J. L. Segura, N. Martín, *Angew. Chem.* **2001**, *113*, 1416–1455; *Angew. Chem. Int. Ed.* **2001**, *40*, 1372–1409.
- [10] a) J. O. Jeppesen, J. Perkins, J. Becher, J. F. Stoddart, *Org. Lett.* **2000**, *2*, 3547–3550; b) J. O. Jeppesen, J. Perkins, J. Becher, J. F. Stoddart, *Angew. Chem.* **2001**, *113*, 1256–1261; *Angew. Chem. Int. Ed.* **2001**, *40*, 1216–1221; c) C. P. Collier, J. O. Jeppesen, Y. Luo, J. Perkins, E. W. Wong, J. R. Heath, J. F. Stoddart, *J. Am. Chem. Soc.* **2001**, *123*, 12632–12641; d) J. O. Jeppesen, J. Becher, J. F. Stoddart, *Org. Lett.* **2002**, *4*, 557–560; e) Y. Luo, C. P. Collier, J. O. Jeppesen, K. A. Nielsen, E. Delonno, G. Ho, J. Perkins, H.-R. Tseng, T. Yamamoto, J. F. Stoddart, J. R. Heath, *ChemPhysChem* **2002**, *3*, 519–525.
- [11] See for example: a) F. Le Derf, E. Levillain, G. Trippé, A. Gorgues, M. Sallé, R. M. Sebastian, A. M. Caminade, J. P. Majoral, *Angew. Chem.* **2001**, *113*, 224–227; *Angew. Chem. Int. Ed.* **2001**, *40*, 224–227; b) F. Le Derf, M. Mazari, N. Mercier, E. Levillain, G. Trippé, A. Riou, P. Richomme, J. Becher, J. Garin, J. Orduna, N. Gallego-Planas, A. Gorgues, M. Sallé, *Chem. Eur. J.* **2001**, *7*, 447–455; c) G. Trippé, E. Levillain, F. Le Derf, A. Gorgues, M. Sallé, J. O. Jeppesen, K. Nielsen, J. Becher, *Org. Lett.* **2002**, *4*, 2461–2464.
- [12] a) J. O. Jeppesen, K. Takimiya, F. Jensen, J. Becher, *Org. Lett.* **1999**, *1*, 1291–1294; b) J. O. Jeppesen, K. Takimiya, F. Jensen, T. Brimert, K. Nielsen, N. Thorup, J. Becher, *J. Org. Chem.* **2000**, *65*, 5794–5805.
- [13] C. Bucher, R. S. Zimmerman, V. Lynch, J. L. Sessler, *J. Am. Chem. Soc.* **2001**, *123*, 9716–9717.
- [14] More than 20 % of **3** can be recovered during chromatographic purification.
- [15] H. Tsukube, H. Furuta, A. Odani, Y. Takeda, Y. Kudo, Y. Inoue, Y. Liu, H. Sakamoto, K. Kimura in *Comprehensive Supramolecular Chemistry*, Vol. 8 (Eds.: J. L. Atwood, J. E. D. Davies, D. D. MacNicol, F. Vögtle, D. Reinhoudt), Pergamon, Oxford, **1996**, pp. 425–482.
- [16] P. Anzenbacher, Jr., K. Jursýková, J. L. Sessler, *J. Am. Chem. Soc.* **2000**, *122*, 9350–9351.
- [17] M. J. Hynes, *J. Chem. Soc. Dalton Trans.* **1993**, 311–312.
- [18] a) J. A. A. de Boer, D. N. Reinhoudt, *J. Am. Chem. Soc.* **1985**, *107*, 5347–5351; b) L. Fielding, *Tetrahedron* **2000**, *56*, 6151–6170.
- [19] Similar results have been observed with Cl<sup>−</sup> ions.
- [20] CV titration experiments were also carried out with solutions containing F<sup>−</sup> ions. However, it was not possible to obtain a Δ*E* value for the **4**·F<sup>−</sup> complex, because the redox events become irreversible. This may be caused by the formation of a N–F bond at the doped state, by delocalization of the positive charge from TTF<sup>+</sup>, or by oxidation of the calix[4]pyrrole skeleton. This phenomena has previously been observed, see ref. [8].
- [21] The control experiments carried out by means of the titration of **3** with solutions containing Br<sup>−</sup> ions did not show any observable displacement of the first oxidation potential.
- [22] The character of the highest-occupied molecular orbital (HOMO) of monopyrrolo TTFs has recently been calculated

- and shows that approximately 13% of the HOMO density is located on the outer pyrrole ring, see ref. [12b].
- [23] P. A. Gale, J. L. Sessler, V. Král, V. Lynch, *J. Am. Chem. Soc.* **1996**, *118*, 5140–5141.
- [24] Binding constants between *meso*-octamethylcalix[4]pyrrole and  $\text{Cl}^-$  and  $\text{F}^-$  ions in  $\text{CD}_3\text{CN}/0.5\%$  v/v  $\text{D}_2\text{O}$  at 295 K have been determined by  $^1\text{H}$  NMR spectroscopy to be  $5.0 \times 10^3 \text{ M}^{-1}$  and  $> 1.0 \times 10^4 \text{ M}^{-1}$ , respectively, see ref. [5a]. However, calorimetric measurements carried out in anhydrous MeCN ( $< 10$  ppm) on *meso*-octamethylcalix[4]pyrrole gave binding constants of  $1.9 \times 10^5 \text{ M}^{-1}$  and  $1.5 \times 10^5 \text{ M}^{-1}$  for  $\text{Cl}^-$  and  $\text{F}^-$  ions, respectively, see ref. [5b].
- [25] To minimize adsorption phenomena, a high scan rate of  $0.5 \text{ V s}^{-1}$  was used.

## Gold/DNA Nanostructures

### Towards Multistep Nanostructure Synthesis: Programmed Enzymatic Self-Assembly of DNA/Gold Systems\*\*

Antonios G. Kanaras, Zhenxin Wang,  
Andrew D. Bates, Richard Cosstick, and  
Mathias Brust\*

The programmed self-assembly of nanostructures from well-defined units is an important aim in nanoscience.<sup>[1,2]</sup> The use of gold nanoparticles stabilized by thiol-modified DNA is a promising approach towards this goal.<sup>[3–8]</sup> The specificity of DNA base-pairing provides a precise means of programming interactions between particles by hybridization with specifically designed linker strands. To introduce an additional level of control, we have developed a general method by which the reactivity of initially latent DNA linking sites can be switched on deliberately. We have adapted well-developed methods of molecular biology to produce a nanoscale analogue of protecting groups. We show that linking sites can be protected by hybridization with complementary strands and deprotect-

ed by cleaving these double strands at predetermined sites with restriction enzymes. This results in cohesive ends of single-stranded DNA, which can bind by hybridization to complementary sequences present in the system. In a second enzymatic step the DNA phosphodiester backbones at the hybridization sites are covalently joined using a DNA ligase. This approach represents a generic protocol that will enable multistep nanostructure syntheses.

In addition to DNA, further biomolecular interactions have been exploited for programmed assembly. These include other specific recognition motifs such as antibody–antigen and biotin–avidin binding.<sup>[8–11]</sup> A number of nonbiomolecular systems with various degrees of complexity have also been reported.<sup>[12–16]</sup> These approaches generally have in common that the reactivity of the binding sites is determined by the initial design of the system. A reaction, once started, proceeds until all reactive sites have been consumed by binding to complementary motifs. This essentially limits programmed nanostructure assembly to single-step reactions. Conversely, modern preparative chemistry is characterized by complex multistep syntheses, which can routinely be carried out by selectively addressing certain reactive sites while others are left temporarily unreactive. This is achieved by the use of protecting groups, which are essential to practically all modern chemical syntheses. Here we introduce a comparable concept to programmed nanostructure assembly, which uses the restriction sites in double-stranded DNA as protected linking motifs and restriction endonucleases as selective deprotecting agents. The complete reaction sequence carried out to demonstrate this principle is illustrated schematically in Figure 1.

The starting point for this work was the preparation of an aqueous solution of 15 nm gold nanoparticles, which were coated and stabilized by a ligand shell of thiol-modified

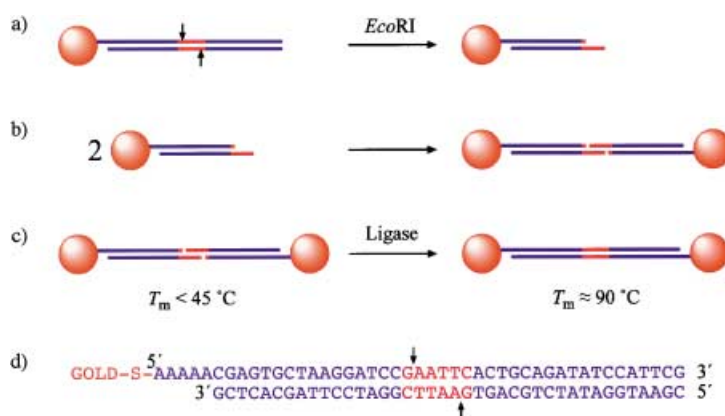


**Figure 1.** Schematic description of the method. a) Gold nanoparticles derivatized with double-stranded DNA are treated with restriction enzyme *EcoRI*, which cleaves the DNA to yield cohesive ends. The red color represents the recognition site of the enzyme, and the arrows indicate the sites of cleavage on each strand. In reality, each 15 nm particle has around 100 DNA ligands; b) Two cohesive ends hybridize, which leads to a weak association of particles; c) The DNA backbones are covalently joined at the hybridized site by DNA ligase to yield a stable 40-base-pair double-stranded link between particles; d) The sequences of the oligonucleotides are illustrated, together with the *EcoRI* site and positions of backbone cleavage, as in (a).

[\*] Dr. M. Brust, A. G. Kanaras, Dr. Z. Wang, Dr. R. Cosstick  
Centre for Nanoscale Science, Department of Chemistry  
The University of Liverpool  
Liverpool L69 7ZD (UK)  
Fax: (+44) 151-794-3588  
E-mail: m.brust@liv.ac.uk

A. G. Kanaras, Dr. A. D. Bates  
School of Biological Sciences  
The University of Liverpool  
Liverpool L69 7ZB (UK)

[\*\*] The authors wish to thank John Naylor for his help with TEM and Dr. Damian Parry for helpful advice. Financial support by the EPSRC, BBSRC, and the European Union (NANOMOL) is gratefully acknowledged. M.B. is the recipient of an EPSRC Advanced Research Fellowship and A.G.K. is partially supported by a University of Liverpool PhD Studentship.